

gion). It is then possible that the initial GRB emission is isotropic and is then collimated by the interaction with a funnel-like medium. This limit on anisotropy allows the determination of the total, isotropic, electromagnetic energy produced by a GRB, which for GRB991216 is  $E > 7.2 \times 10^{52} \text{ erg s}^{-1} = 0.04 M_{\odot} c^2$ . Another important implication of the previous limit is on the iron abundance of the medium, which must be much higher than solar ( $X_{\text{Fe}} > 60$ ). This high value of the iron abundance indicates that the ejecta were—at some stage of the progenitor evolution—produced by a supernova explosion (30, 31).

In conclusion, the most straightforward scenario that emerges from all the pieces of evidence we have gathered is the following. A massive progenitor—like a hypernova or a collapsar (32, 33)—ejects, shortly before the GRB, a substantial fraction of its mass. This event is similar to a supernova explosion, as in the case of the SupraNova model (34).

References and Notes

1. C. L. Fryer, S. E. Woosley, D. H. Hartman, *Astrophys. J.* **526**, 152 (1999).
2. P. Mészáros, M. J. Rees, *Mon. Not. R. Astron. Soc.* **299**, L10 (1998).
3. M. Boettcher, C. D. D. Dermer, A. W. Crider, E. D. Liang, *Astron. Astrophys.* **343**, 111 (1999).
4. R. Perna, A. Loeb, *Astrophys. J.* **501**, 467 (1998).
5. R. A. M. J. Wijers, T. J. Galama, *Astrophys. J.* **523**, 177 (1999).
6. R. Sari, T. Piran, R. Narayan, *Astrophys. J.* **497**, L17 (1998).
7. D. Lazzati, G. Ghisellini, S. Campana, *Mon. Not. R. Astron. Soc.* **304**, L31 (1999).
8. M. Vietri, G. C. Perola, L. Piro, L. Stella, *Mon. Not. R. Astron. Soc.* **308**, L29 (2000).
9. C. Weth, P. Meszaros, T. Kallman, M. Rees, *Astrophys. J.* **534**, 581 (2000).
10. M. Boettcher, C. L. Fryer, in preparation (available at <http://xxx.lanl.gov/abs/astro-ph/0006076>).
11. L. Piro et al., *Astrophys. J.* **514**, L73 (1999).
12. A. Yoshida et al., *Astron. Astrophys.* **138**, 433 (1999).
13. Y. Daisuke et al., *Publ. Astron. Soc. Japan* **52**, 509 (2000).
14. S. R. Kulkarni et al., *Proc. 5th Huntsville GRB Symposium*, in press (available at <http://xxx.lanl.gov/abs/astro-ph/0002168>).
15. M. C. Weisskopf, S. O'Dell, L. P. van Speybroeck, *Proceedings of Multilayer and Grazing Incidence X-Ray/EUV Optics III*, R. B. Hoover, A. B. Walker, Eds. (SPIE Press, Bellingham, WA, 1996), p. 2.
16. R. M. Kippen, R. D. Preece, T. Giblin, *GCN Circular* **463** (2000); *GCN Circular* **504** (2000).
17. T. Takeshima, C. Markwardt, F. Marshall, T. Giblin, R. M. Kippen, *GCN Circular* **478** (2000).
18. K. Hurley et al., *GCN Circular* **484** (2000); *GCN Circular* **505** (2000).
19. L. Piro et al., *GCN Circular* **500** (2000).
20. J. P. Halpern et al., *Astrophys. J.*, in press (available at <http://xxx.lanl.gov/abs/astro-ph/0006206>).
21. D. A. Frail et al., *Astrophys. J.*, in press (available at <http://xxx.lanl.gov/abs/astro-ph/0003138>).
22. L. Piro, *Proceedings of UV and X-ray Spectroscopy of Laboratory and Astrophysical Plasmas*, E. Silver, S. Kahn, Eds. (Cambridge Univ. Press, Cambridge, 1993), p. 448.
23. F. Paerels, E. Kuulkers, J. Heise, J. in 't Zand, D. Liedahl, *Astrophys. J.* **535**, L25 (2000).
24. L. Amati et al., *Science* **290**, 953 (2000).
25. T. R. Kallmann, R. McCray, *Astrophys. J. Suppl. Ser.* **50**, 263 (1983).
26. P. M. Vreeswijk et al., *GCN Circular* **496** (2000).
27. S. G. Djorgovski et al., *GCN Circular* **510** (2000).
28. The common-envelope phase happens when the hydrogen envelope of the secondary star expands, engulfing the compact primary (neutron star or black hole). Friction and tidal forces cause the compact object to spiral in the giant's core, ejecting the hydrogen envelope preferentially along the orbital plane, forming a disk [E. Sandquist, R. E. Taam, X. Chen, P. Bodenheimer, A. Burkert, *Astrophys. J.* **500**, 909 (1998)].

29. The beaming factor  $\Delta\Omega/4\pi$  is the fraction of sky over which GRB photons are emitted. It is equal to 1 if the emission is isotropic and  $\approx \theta^2/4$  in the case of a jet with opening angle  $\theta$ .
30. S. E. Woosley, T. A. Weaver, *Astrophys. J. Suppl. Ser.* **101**, 181 (1995).
31. P. Bouchet et al., *Astron. Astrophys.* **245**, 490 (1991).

32. B. Paczynski, *Astrophys. J.* **494**, L45 (1998).
33. S. E. Woosley, *Astrophys. J.* **405**, 273 (1993).
34. M. Vietri, L. Stella, *Astrophys. J.* **507**, L45 (1998).
35. See Chandra calibration reports (<http://asc.harvard.edu/cal>).
36. We thank the Chandra team for support, in particular F. Nicastro and A. Fruscione for help in data reduction; M. Boettcher for critical suggestions; G. Ricker for useful discussions on the observational strategy; and L. A. Antonelli for comments. Supported by NASA contract NAS8-39073 to the Chandra X-ray Center (M.G.).

5 September 2000; accepted 10 October 2000

## Mode-Specific Energy Disposal in the Four-Atom Reaction $\text{OH} + \text{D}_2 \rightarrow \text{HOD} + \text{D}$

Brian R. Strazisar, Cheng Lin, H. Floyd Davis\*

Experiments, employing crossed molecular beams, with vibrational state resolution have been performed on the simplest four-atom reaction,  $\text{OH} + \text{D}_2 \rightarrow \text{HOD} + \text{D}$ . In good agreement with the most recent quantum scattering predictions, mode-specific reaction dynamics is observed, with vibration in the newly formed oxygen-deuterium bond preferentially excited to  $v = 2$ . This demonstrates that quantum theoretical calculations, which in the past decade have achieved remarkable accuracy for three-atom reactions involving three dimensions, have progressed to the point where it is now possible to accurately predict energy disposal in four-atom reactions involving six dimensions.

A central goal in the study of chemical reaction dynamics is to understand the details of how bonds are broken and formed during a reaction (1). The potential energy surface (PES), which describes how the potential energy of the system depends on the relative position of the atoms, may be derived using ab initio or density functional theory (2). Classical, quasi-classical, or quantum scattering calculations may be carried out using the PES to understand which collision geometries and forms of reactant energy (such as translational or vibrational) facilitate passage through the transition state region to the chemical products (3, 4). Scattering calculations can also predict product quantum state distributions as a function of scattering angle (3, 4).

The accuracy of theoretical calculations may be tested by comparing predicted product quantum state and angular distributions to those measured experimentally (3–5). To date, studies of three-atom systems ( $\text{A} + \text{BC} \rightarrow \text{AB} + \text{C}$ ), using crossed molecular beams, have provided the most detailed insight into the mechanisms and energy disposal in chemical reactions (5–11). Recent studies of the  $\text{H} + \text{D}_2 \rightarrow \text{HD} + \text{D}$  (6, 7) and  $\text{O} + \text{H}_2 \rightarrow \text{OH} + \text{H}$  (11) reactions have employed the

high-resolution H atom Rydberg tagging method (12) to determine the vibrational and rotational energy distributions of the diatomic products as a function of scattering angle.

A more recent challenge to both theoreticians and experimentalists has been the study of four-atom reactions ( $\text{AB} + \text{CD} \rightarrow \text{ABC} + \text{D}$  or  $\text{ABC} + \text{D} \rightarrow \text{AB} + \text{CD}$ ). In three-atom systems, internal excitation is limited to two rotational and one vibrational degree of freedom in the diatomic reactant and product. In four-atom reactions, the triatomic reactant or product (if nonlinear) has three vibrational degrees of freedom, some involving motion of the newly broken or formed bond. When a triatomic molecule is produced in a four-atom reaction, it becomes possible to ask not only how much energy is deposited into product vibration, but also how energy is distributed among the vibrational modes.

Mode-specific behavior is an important feature of reaction dynamics involving four-atom systems. Excitation of the OH stretching mode of  $\text{H}_2\text{O}$  greatly enhances the rate of the  $\text{H} + \text{H}_2\text{O} \rightarrow \text{OH} + \text{H}_2$  reaction, whereas excitation of the  $\text{H}_2\text{O}$  bending mode has no effect (13, 14). In the  $\text{H} + \text{HOD}$  reaction, selective excitation of either the OH or OD stretching overtone (13) or fundamental (15) in HOD can dictate which bond is reactive. From the principle of microscopic reversibility, preferential vibrational excitation of the new bond in the reverse reaction might be

Department of Chemistry and Chemical Biology, Cornell University, Ithaca, NY 14850, USA.

\*To whom correspondence should be addressed. E-mail: hfd1@cornell.edu

anticipated. However, earlier scattering calculations on two different PESs showed no evidence for mode-specific energy disposal (16, 17). Instead, the HOD was predicted to be produced in a range of vibrational states, with no clear preference for particular HOD bending or OD stretching levels. In contrast, very recent quantum scattering calculations (18) on a new PES (19) predicted highly mode-specific energy disposal with preferential vibrational excitation of the newly formed OD bond to  $\nu = 2$ .

The  $\text{OH} + \text{H}_2 \rightarrow \text{H}_2\text{O} + \text{H}$  reaction is the primary source of water in the combustion of hydrogen (20). It is also important in interstellar chemistry as the regenerative step in the OH maser and the active medium in the  $\text{H}_2\text{O}$  maser (21). It is a prototype reaction for H atom abstraction by OH radicals leading to water production. The reaction has become the most important four-atom benchmark, and calculations of the reactive PES have been performed with increasing sophistication (16–19, 22, 23). Previously, the most detailed experimental insight into the mechanism came from an experiment using crossed molecular beams, in which the HOD product from the  $\text{OH} + \text{D}_2 \rightarrow \text{HOD} + \text{D}$  reaction was detected (17). The HOD was found to be strongly backward scattered with respect to the initial OH direction, indicating a direct mechanism, with the O atom in OH abstracting a D atom from  $\text{D}_2$  via a nearly collinear O–D–D geometry. Although 64% of the available energy was channeled into HOD internal excitation, it was not clear how this energy was distributed.

Our experimental apparatus consists of two fixed, pulsed molecular beams and a rotatable detector assembly housed within a large vacuum chamber. The OH radicals were produced by photodissociation (at 193-nm wavelength) of anhydrous nitric acid (24) seeded in a pulsed supersonic expansion of hydrogen at 2 atm (1 atm = 101.3 kPa) (25). The measured velocity of the OH beam was 3340 m/s, and the rotational temperature (characterized using laser-induced fluorescence) was  $\sim 85$  K. The  $\text{D}_2$  beam was produced by pulsed supersonic expansion of 20%  $\text{D}_2$  seeded in  $\text{H}_2$  (5-atm total pressure) and characterized using 2+1 resonance-enhanced multiphoton ionization (26). The  $\text{D}_2$  velocity was 2416 m/s and the rotational temperature was  $\sim 130$  K.

The beams were collimated by skimmers and crossed at  $90^\circ$  in a separately pumped scattering chamber. From the measured beam characteristics, the average collision energy was  $6.6 \pm 0.5$  kcal/mol (half width at half maximum), nearly identical to the 6.3 kcal/mol used previously in experimental (17) and theoretical (17, 18) studies. Pulsed lasers operating at 121.6 and 365.6 nm were used to excite nascent D atoms at the interaction region to a high-lying Rydberg state ( $n = 40$ ). The “tagged” D atom

products evolved spatially through a distance of 29.2 cm to a detector where they were field-ionized and collected on a microchannel plate (12). The detector assembly may be rotated within the plane of the beams to obtain a full angular distribution of the products. For this collision energy, data was acquired at 14 laboratory angles.

The energetics of the reaction are shown in Fig. 1, along with the HOD product vibrational energy levels accessible under our experimental conditions. It is believed that the OH bond acts as a “spectator” (22), with the bond length remaining essentially unchanged throughout the course of the reaction. Therefore, only the “active” modes—that is, the HOD bending and the OD local stretching modes—are included (17).

Our observations are in good agreement with the earlier experimental findings that the HOD products are strongly backward scattered from a direct rebound reaction, with a large fraction of available energy deposited into HOD internal excitation (17). The higher resolution of our experiment allows us to gain much more quantitative insight into the disposal of energy into the various vibrational modes of HOD. The D atom time-of-flight (TOF) spectra are dominated by two peaks (Fig. 2). From conservation of energy and momentum, the faster and slower peaks correspond to one and two quanta of excitation in the OD local stretching mode, respectively [(0,1) and (0,2)]. A smaller feature appearing between these peaks corresponds to one quantum of OD stretching and one quantum of HOD bending excitation

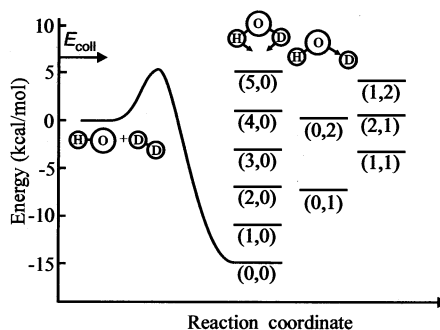


**Fig. 1.** Energy level diagram for the  $\text{OH} + \text{D}_2 \rightarrow \text{HOD} + \text{D}$  reaction. Vibrational levels of the HOD product are labeled  $(m,n)$ , where  $m$  is the quantum number for the bending mode and  $n$  that for the OD local stretching mode.

**Table 1.** Energy disposal into HOD + D products.

Parameter	HOD vibrational level			
	(0,0)	(0,1)	(1,1)	(0,2)
Total population	3%	30%	11%	56%
Total available energy (kcal/mol)	21.2	13.4	9.5	5.9
Average translational energy (kcal/mol)	16.0	10.1	7.1	4.1
Average rotational energy (kcal/mol)	5.2	3.3	2.4	1.7

(1,1). A very small, fast contribution indicates a small yield of vibrationless HOD (0,0). The OD vibrational frequency in HOD is nearly double the bending frequency, and it is therefore impossible to distinguish some of the very closely lying levels (0,1 from 2,0; 1,1 from 3,0; and 0,2 from 2,1 and 4,0). However, recent theoretical calculations (18) predict that only the four vibrational levels noted above are significantly populated.

The solid lines in each TOF spectrum (Fig.

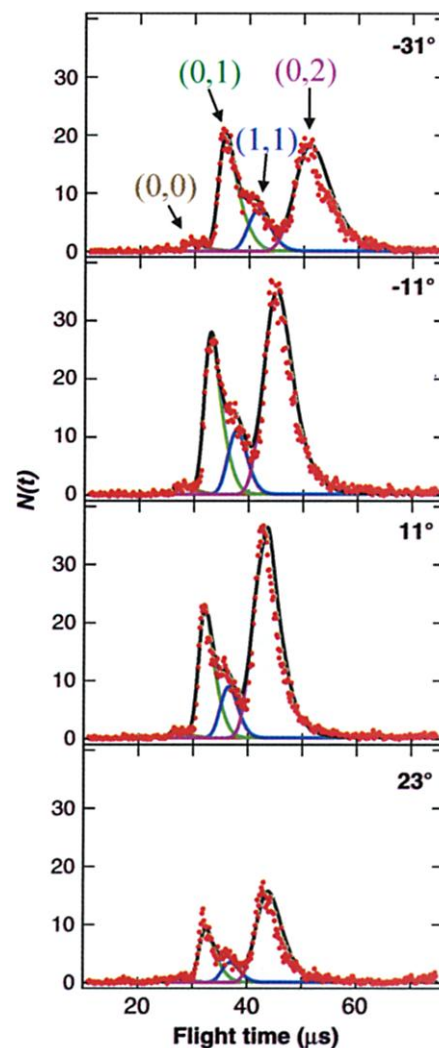


**Fig. 2.** D atom product time-of-flight spectra at four selected laboratory angles relative to the OH initial velocity vector. Solid lines represent simulations based on best-fit translational energy and angular distributions.

2) correspond to simulated spectra based on a forward convolution calculation using a separate translational energy distribution  $[P(E)]$  and center-of-mass angular distribution  $[T(\theta)]$  for each of the four populated HOD vibrational energy levels. The simulations explicitly include averaging effects due to the finite angular divergences of the beams, the velocity distributions of the reactants, and the distribution of collision energies. After optimizing the simulations to agree with our experimental TOF data, we directly transformed the  $P(E)$  and  $T(\theta)$  distributions to velocity space to obtain a D atom product center-of-mass flux contour map (Fig. 3). We also extracted relative populations for each vibrational state and the average amount of rotational energy for each individual vibrational level. Approximately 37% of the total available energy goes into translation, in close agreement with the results of Alagia *et al.*, who measured 34% (17). By comparing the average translational energy to the total energy available for each vibrational level, we determined that 58% of the total energy is deposited into HOD vibration and 5% into HOD rotation. The HOD vibrational populations and average translational and rotational energies in each vibrational state (Table 1) show that this reaction exhibits highly mode-specific behavior, with the newly formed OD bond preferentially vibrationally excited. This is consistent with theoretical calculations, which indicate that the OD bond is significantly longer in the transition state (1.36 Å) than in the HOD product (0.957 Å) (19). Relatively little excitation of the bending mode is observed because the transition state HOD angle (97.1°) is only slightly smaller than that of the product (104.5°) (19). As noted previously, the OH stretch is not excited because this spectator bond length remains essentially un-

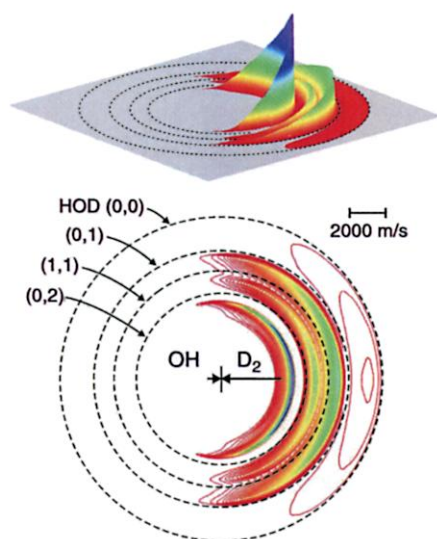


**Fig. 3.** D atom product flux contour map and surface plot in center of mass velocity space. Dashed circles represent the maximum velocity of D atoms recoiling from HOD in indicated vibrational states.

changed throughout the reaction.

Product vibrational state populations are an extremely sensitive test of calculated reactive PESs. We compared our results to theoretical predictions based on scattering calculations, using three progressively newer PESs (Fig. 4). The three calculated vibrational energy distributions (Fig. 4, A through C) were obtained from quantum scattering calculations using the rotating bond approximation (18), which involves treating the HOD bending and OD stretching vibrations with explicit quantum mechanics, whereas the other degrees of freedom are treated approximately. As the PESs have improved over the past few decades, the predicted HOD product vibrational distributions have changed quite significantly. The first vibrational distribution (Fig. 4A) was calculated using the first analytical OH + H<sub>2</sub> PES by Schatz and Elgersma (SE), published in 1980 (16). This surface is a many-body expansion fit

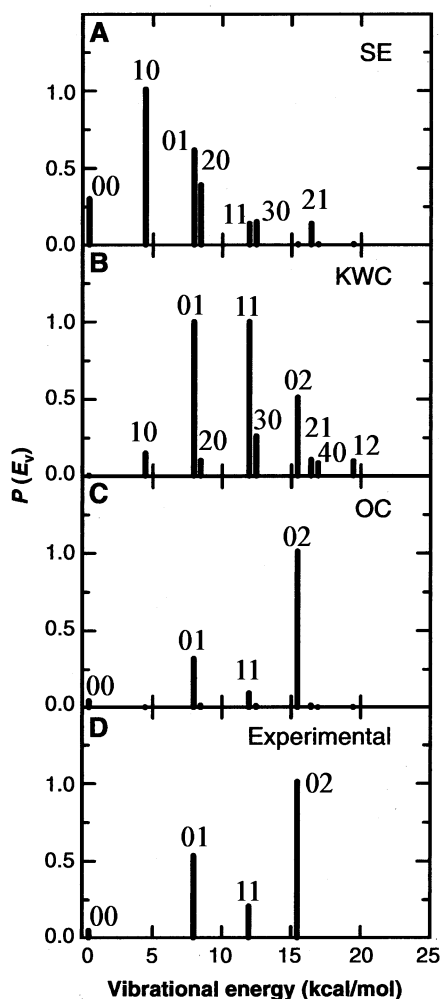


**Fig. 4.** Comparison of three different theoretical predictions (A to C) of HOD vibrational energy distributions (17, 18) to experimental measurements (D). Theoretical predictions are based on rotating bond approximation calculations on the SE (16), KWC (17), and OC (19) potential at  $E_{\text{coll}} = 6.3$  kcal/mol.

to the somewhat limited ab initio data available at the time. This surface has been used extensively for many years, and has therefore been subject to a great deal of scrutiny. Most notably, the transition state has a considerably shorter OD bond length than predicted by more recent calculations, leading to much less OD stretch excitation in the products. The second distribution (Fig. 4B) is from a more recent PES calculated by Kliesch, Werner, and Clary (KWC) (17). This surface was generated by a reduced dimensionality fit to newer, more extensive ab initio data. To simplify the fitting of the surface to the ab initio points, the “spectator” OH bond distance and the out-of-plane angle away from the transition state were held constant. The agreement with our data is slightly better because more vibrational excitation of HOD is predicted. The prediction does not, however, reflect the mode-specific behavior observed experimentally. The third calculated vibrational energy distribution (Fig. 4C) was obtained from recent quantum scattering calculations (18) using a new PES by Ochoa de Aspuru and Clary (OC) (19) generated from a full six-dimensional fit to the same ab initio data used for the KWC potential. The predicted vibrational distribution from the OC PES agrees quite well with our experimental measurements (Fig. 4D).

Our experimental results demonstrate that modern quantum scattering calculations, previously verified only for three-atom systems in three dimensions, are now able to accurately predict vibrational energy disposal in much more complex four-atom reactions involving six dimensions (4, 18).

#### References and Notes

1. R. D. Levine, R. B. Bernstein, *Molecular Reaction Dynamics and Chemical Reactivity* (Oxford Univ. Press, Oxford, 1987).
2. T. H. Dunning, Ed., *Advances in Molecular and Electronic Structure Theory* (Jai Press, Greenwich, CT, 1990), vol. 1.
3. G. C. Schatz, *J. Phys. Chem.* **100**, 12839 (1996).
4. D. C. Clary, *Science* **279**, 1879 (1998).
5. P. Casavecchia, *Rep. Prog. Phys.* **63**, 355 (2000).
6. L. Schnieder *et al.*, *Science* **269**, 207 (1995).
7. L. Schnieder, K. Seekamp-Rahn, E. Wrede, K. H. Welge, *J. Chem. Phys.* **107**, 6175 (1997).
8. M. Alagia *et al.*, *Science* **273**, 1519 (1996).
9. D. M. Neumark, A. M. Wodtke, G. N. Robinson, C. C. Hayden, Y. T. Lee, *J. Chem. Phys.* **82**, 3045 (1985).
10. M. Alagia *et al.*, *J. Chem. Phys.* **108**, 6698 (1998).
11. X. Liu, J. J. Lin, S. Harich, G. C. Schatz, X. Yang, *Science* **289**, 1536 (2000).
12. L. Schnieder, W. Meier, K. H. Welge, M. N. R. Ashfold, C. M. Western, *J. Chem. Phys.* **92**, 7027 (1990).
13. A. Sinha, M. C. Hsiao, F. F. Crim, *J. Chem. Phys.* **94**, 4928 (1991).
14. M. J. Bronikowski, W. R. Simpson, R. N. Zare, *J. Phys. Chem.* **97**, 2204 (1993).
15. ———, *J. Phys. Chem.* **97**, 2194 (1993).
16. G. C. Schatz, H. Elgersma, *Chem. Phys. Lett.* **73**, 21 (1980).
17. M. Alagia *et al.*, *Chem. Phys.* **207**, 389 (1996).
18. S. K. Pogrebnya, J. Palma, D. C. Clary, J. Echave, *Phys. Chem. Chem. Phys.* **2**, 693 (2000).
19. G. Ochoa de Aspuru, D. C. Clary, *J. Phys. Chem. A* **102**, 9631 (1998).
20. J. Warnatz, in *Combustion Chemistry*, W. C. Gardiner, Ed. (Springer-Verlag, New York, 1984), chap. 5.
21. T. J. Millar, D. A. Williams, Eds., *Rate Coefficients in*

- Atmospheric Chemistry* (Kluwer, Dordrecht, Netherlands, 1988).
22. S. P. Walch, T. H. Dunning Jr., *J. Chem Phys.* **72**, 1303 (1980).
23. K. Kudla and G. C. Schatz, in *The Chemical Dynamics and Kinetics of Small Radicals*, K. Liu, A. Wagner, Eds. (World Scientific, Singapore, 1995).
24. G.-H. Leu, C.-W. Hwang, I.-C. Chen, *Chem. Phys. Lett.* **257**, 481 (1996).
25. The OH radicals were produced exclusively in their

ground vibrational state. Both O(<sup>1</sup>D) and H atoms were also produced to some extent. However, O(<sup>1</sup>D) is efficiently consumed by the H<sub>2</sub> carrier gas, and the 9.6 kcal/mol potential energy barrier for H + D<sub>2</sub> → HD + D is far higher than the experimental collision energy. In order to surmount the potential energy barrier for reaction, the collision energy was increased by passing the HNO<sub>3</sub>/H<sub>2</sub> mixture through a resistively heated stainless steel tube mounted to the end of the pulsed nozzle.

26. K.-D. Rinnen, M. A. Buntine, D. A. V. Kliner, R. N. Zare, W. M. Huo, *J. Chem. Phys.* **95**, 214 (1991).
27. This research was supported by the U.S. Department of Energy and by the Alfred P. Sloan Foundation. B.R.S. was supported by a graduate fellowship from Eastman Kodak. We thank H. U. Stauffer for writing the data analysis software.

17 July 2000; accepted 29 September 2000

# First-Principles Theory for the H + H<sub>2</sub>O, D<sub>2</sub>O Reactions

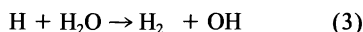
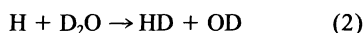
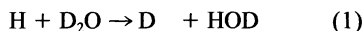
Dong H. Zhang,<sup>1\*</sup> Michael A. Collins,<sup>3</sup> Soo-Y. Lee<sup>2</sup>

A full quantum dynamical study of the reactions of a hydrogen atom with water, on an accurate ab initio potential energy surface, is reported. The theoretical results are compared with available experimental data for the exchange and abstraction reactions in H + D<sub>2</sub>O and H + H<sub>2</sub>O. Clear agreement between theory and experiment is revealed for available thermal rate coefficients and the effects of vibrational excitation of the reactants. The excellent agreement between experiment and theory on integral cross sections for the exchange reaction is unprecedented beyond atom-diatom reactions. However, the experimental cross sections for abstraction are larger than the theoretical values by more than a factor of 10. Further experiments are required to resolve this.

Since molecular beam experiments first examined chemical reactions at the most rigorous elementary level (1), there has been intense effort to develop theory for reliable calculations of chemical dynamics. The purpose of this quest for quantitatively accurate theory is to provide a definitive understanding of the mechanisms of chemical reactions—an understanding that will ultimately provide the basis for confident prediction of chemical rates and for control of chemical reactions.

Quantitative theory faces two difficult tasks: the construction of accurate multidimensional potential energy surfaces (PESs) and the performance of reactive scattering calculations on these surfaces. These tasks have been largely achieved for triatomic systems (2, 3), in particular for the H + H<sub>2</sub> reaction family (4, 5). Accurate theory for tetraatomic reactions should substantially extend our understanding of elementary reaction mechanisms (3, 6). Four-atom systems support a much richer variety of phenomena, including competing reaction pathways, steric hindrance, and the influence of different reactant vibrations on the course of the reaction. Over the past several years, advances in accurate reactive scattering calculations (7–9) and the construction of PESs

(10–14) have been combined with the rise in computational power to make accurate ab initio dynamics practicable for four-atom systems. This study reports such calculations for the H + H<sub>2</sub>O family



These reactions have become the prototype tetraatomic reactions, in which different vibrational modes in the reactants can play an important role in the reaction dynamics (1). This role has been extensively studied in the past decade (15–23). In addition, the thermal rate coefficient for reaction 3 is known (24), and the effect of reactant translational energy on reactions 1 and 3 has been closely examined (25–29). Because this system has few electrons and three very light atoms, it is an ideal candidate for the theoretical study of tetraatomic reactions in terms of both practicality and importance. Not surprisingly, these reactions, and the reverse reaction of OH + H<sub>2</sub>, have been the focus of the development of quantum reaction dynamics for four-atom systems (6–9, 30–32). Once substantial progress had been made with the scattering methodology, attention naturally turned to improving the PES (33–35). However, only very recently have PESs been developed that can accurately describe reactions 1 to 3, including the effect of vibrationally excited reactants (14). We briefly describe the methods used to obtain “benchmark” descriptions of reactions 1 to 3. The calculations are then

compared with the available experimental data to see what stage theory has reached. It will become clear that the substantial amount of computer time expended here was necessary to approach “chemical accuracy,” as measured by some types of experimental data. In one case, the theory is sufficiently reliable to suggest that some experimental data ought to be reconsidered.

The PES is constructed as an interpolation of high-level ab initio quantum chemistry data (36) evaluated over a large range of molecular geometries. This interpolation scheme for PES (10–12) has been demonstrated to be sufficiently accurate for quantum scattering (13, 14). The quantum chemistry calculations are discussed in a recent paper (14). A data set of 1000 geometries was constructed (which required ~800 days of CPU time on a state-of-the-art workstation). In contrast to earlier work (14), no additive or scaling approximations have been employed here. The resulting PES is depicted schematically in Fig. 1. When the total angular momentum  $J = 0$ , the exact quantum dynamics of the molecule is calculated by using a time-dependent wave packet method (8), extended so that the exact total probabilities for reactions 1 to 3 could be evaluated with all six internal degrees of freedom taken into account explicitly. For  $J > 0$ , the centrifugal sudden (CS) approximation is used (which should only introduce a few-percent error in the total reaction cross sections at medium to high translational energy) (9).

In Fig. 2, we compare theoretical integral cross sections for the exchange reaction with the experimental results (28, 29): the absolute cross sections at a relative translational energy of 1.5 and 2.2 eV and the excitation function of the reaction in the line-of-center functional model (29). The first-principles theoretical results agree excellently with the experiments in all respects. We note that the experimental result is thermally averaged over the initial rotation of D<sub>2</sub>O, whereas the theoretical result is for initial nonrotating D<sub>2</sub>O (preliminary calculations showed that rotational excitation of the triatomic reactant has no substantial effect on the integral cross section).

The agreement between theory and experiment for the abstraction reactions is both positive and negative. A comparison of the experimental data (24) with the theoretical

<sup>1</sup>Department of Computational Science, <sup>2</sup>Department of Chemistry, National University of Singapore, Singapore 119260. <sup>3</sup>Research School of Chemistry, Australian National University, Canberra, ACT 0200, Australia.

\*To whom correspondence should be addressed. E-mail: zhangdh@cz3.nus.edu.sg